scRNA-Sequencing uncovers a TCF-4-dependent transcription factor network regulating commissure development

Marie-Theres Wittmann,[1] Philipp Kirchner,[1] Arif B. Ekici,[1] Elisabeth Sock,[2] D. Chichung Lie,[2,3] André Reis[1,3] *

[1]Institute of Human Genetics, Universitätsklinikum Erlangen, Friedrich-Alexander-Universität Erlangen-Nürnberg (FAU), Erlangen, 91054, Germany

[2]Institute of Biochemistry, Emil Fischer Center, Friedrich-Alexander-Universität Erlangen-Nürnberg, 91054, Germany

[3] These authors contributed equally to this work

[*] Correspondence: andre.reis@uk-erlangen.de

* Corresponding author:

Prof. Dr. André Reis

Institute of Human Genetics

Universitätklinikum Erlangen

Friedrich-Alexander-Universität Erlangen-Nürnberg

91054 Erlangen

Germany

E-mail: andre.reis@uk-erlangen.de

Running title: Transcription factor 4 in forebrain development

Abstract

Text body

References

Figures

Supplemental tables

Abstract

Intercortical connectivity is important for higher cognitive brain functions by providing the basis for integrating information from both hemispheres. We show that ablation of the neurodevelopmental disorder associated bHLH factor *Tcf4* results in complete loss of forebrain commissural systems in mice. Applying a new bioinformatic strategy integrating transcription factor expression levels and regulon activities from single cell RNA-sequencing data predicted a TCF-4 interacting transcription factor network in intercortical projection neurons regulating commissure formation. This network comprises a number of regulators previously linked to the pathogenesis of intellectual disability, autism-spectrum disorders and schizophrenia, e.g. *Foxg1, Sox11* and *Brg1*. Furthermore, we demonstrate that TCF-4 and SOX11 biochemically interact and cooperatively control commissure formation *in vivo*, and regulate the transcription of genes implied in this process. Our study provides a regulatory transcriptional network for the development of interhemispheric connectivity with potential pathophysiological relevance in neurodevelopmental disorders.

Introduction

Cognitive abilities are highly dependent on the establishment of proper neuronal connectivity between different brain regions and its cellular components (Constantinidis and Klingberg 2016; Hedden and Gabrieli 2004). The corpus callosum, the anterior commissure, and the hippocampal commissure, carry axons across the midline and ensure information flow and coordination between the cerebral hemispheres. Of these, the corpus callosum (CC) is the largest commissural tract of the human brain (Tomasch 1954). Callosal connections serve to integrate and coordinate of sensory-motor functions from the right and left side of the body and are integral to high-level cognitive functions including language, abstract reasoning and high-level associative function (Paul et al. 2007).

Mutations in a number of factors controlling developmental processes such as neuronal precursor proliferation, fate specification, migration and axon guidance, are associated with structural anomalies of commissures (Edwards et al. 2014; Lindwall et al. 2007; Paul et al. 2007; Richards et al. 2004), illustrating that commissure development is highly dependent on the expression of complex genetic programs. Orchestration of the precise temporo-spatial execution of developmental programs is most likely achieved by cell-type specific combinatorial activity of transcription factors. However, information on the composition of transcription factor networks in commissural development remains scarce and is largely confined to the regulation of upper layer neuron specification, which is highly reliant on a SATB2-dependent genetic network (Alcamo et al. 2008; Britanova et al. 2008).

The class I basic helix-loop-helix (bHLH) transcription factor (TF) TCF-4 (transcription factor 4) has recently emerged as a critical transcriptional regulator in forebrain development. Variants in *TCF4* have been associated with schizophrenia, autism and intellectual disability and *TCF4* haploinsufficiency causes the neurodevelopmental disorder Pitt-Hopkins syndrome (PTHS) (OMIM 610954) (Amiel et al. 2007; De Rubeis et al. 2014; Navarrete et al. 2013; Schizophrenia Psychiatric Genome-Wide Association Study 2011; Schizophrenia Working Group of the Psychiatric Genomics 2014; Stefansson et al. 2009; Steinberg et al. 2011; Zweier et al. 2007).

Alterations of TCF-4 dosage in mice lead to disruptions in neocortical neuronal migration, specification of neuronal subtypes, dendrite and synapse formation (Li et al. 2019; Page et al. 2017). Most notably, *TCF4* haploinsufficiency in human and

mice is associated with callosal dysgenesis indicating that *Tcf4* is part of a conserved genetic network controlling the formation of callosal connections (Jung et al. 2018).

TCF-4 belongs to the class I basic basic Helix-Loop-Helix (bHLH) transcription factor family and its transcriptional output is highly dependent on its interaction partners. Traditionally, it is assumed that TCF-4 executes its function through dimerization with proneural class II bHLH TFs (Bertrand et al. 2002; Massari and Murre 2000). A recent *in vitro* study, however, proposed that TCF-4 may be able to interact with a variety of transcriptional regulators outside of the traditional interaction partners of the bHLH class (Moen et al. 2017). TCF-4-interacting transcription factors in the regulation of interhemispheric connectivity have not been identified. Such identification is hampered by the technical challenges to perform unbiased in vivo interactome analyses in a cell type specific manner.

Here, we generated homozygote *Tcf4* knockout (*Tcf4KO*) mice to further validate the role of TCF-4 in the establishment of interhemispheric connectivity. We report that loss of *Tcf4* results in the complete agenesis of forebrain commissures. Using single-cell RNA sequencing (scRNA-seq) followed by the integration of transcription factor expression levels and regulon activities we uncover a TCF-4 interacting transcription factor network for commissure development in *Satb2* expressing neurons. Surprisingly, this transcription factor network involves numerous transcription factors outside the bHLH class. Similar to TCF-4, these interactors are often associated to neurodevelopmental disorders such as intellectual disability, autism and schizophrenia. Further analysis of the interaction between TCF-4 and the regulator SOX11 uncovered a synergistic effect on anterior commissure (AC) and CC formation. Collectively, our findings provide insight into a novel gene regulatory network controlling commissure formation and potentially involved as a common pathogenic pathway in neurodevelopmental and neuropsychiatric diseases.

Results

Tcf4 knockout abolishes commissure development

Tcf4 haploinsufficient mice generated by an insertion of a lacZ/neomycin cassette before exon 4 (Figure 1A) show dysgenesis of the corpus callosum (Jung et al. 2018). To further examine the critical role of *Tcf4* in development of interhemispheric connectivity, we generated *Tcf4* homozygote knockout mice. Effectiveness of the

Tcf4 knockout was assessed by western blot as there are *Tcf4* isoforms with transcriptional start sites after exon 4 (Sepp et al. 2011). Our analysis confirmed the loss of the longest TCF-4 isoform (TCF-4B) in the knockout; expression of a shorter isoform (TCF-4A) persisted (Figure 1B). Despite the residual TCF-4 expression, *Tcf4KO* mice died shortly after birth, indicating the importance of the long TCF-4 isoform during development.

The most striking feature of P0 KO brains was the absence of the forebrain commissure system, i.e. CC, AC, and hippocampal commissure (Figure 1C, D). Staining for the upper layer and interhemispheric projection neuron marker SATB2 (Alcamo et al. 2008; Britanova et al. 2008) revealed a significant increase in SATB2 positive neurons (SATB2+ cells/800µm VZ: WT 1146 ± 75.89; KO 1389 ± 92.45; p = 0.0079), which appeared to be generated at the expense of CTIP2 (CTIP2+ /800µm VZ: WT 691 ± 64.2; KO 476 ± 33.9; p = 0.0079) but not of TBR1 positive deep layer neurons (TBR1+ cells/800µm VZ: WT 695 ± 35.5; KO 540 ± 97.7; p = 0,0556; Figure 1E). These data indicate that the commissure forming SATB2+ neurons were in principle generated in *Tcf4KO* mice. Analysis with the anterograde lipohilic tracer DiI indicated that neurons in *Tcf4KO* mice extended their axons towards the midline yet were unable to cross to the contralateral side (Figure 1D). Staining for GAP43, a marker for the axonal growth cone verified this observation (Figure 1F).

Callosal agenesis can be the consequence of dysfunctional midline generation and fusion (Richards et al. 2004). We analysed mice at E16.5, to investigate the characteristic detachment of extensions to the pial surface by GFAP-expressing glial wedge glia and the presence of Calretinin-expressing guidepost neurons (Paul et al. 2007). At E16.5 both cell types were detected at the midline in *Tcf4KO* mice and no general defect in the organization of the structure was observed (Figure 1G and H), suggesting that the midline had been properly formed.

Tcf4 **knockout dysregulates genes involved in neuronal differentiation and axon guidance**

The presence of SATB2 positive neurons and the formation of a midline in *Tcf4KO* mice raised the possibility that TCF-4 may regulate in particular the formation of the axonal tracts by SATB2 expressing neurons. To identify downstream targets and pathways of TCF-4 in the control of forebrain commissure formation, scRNA-seq was conducted from E18.5 neocortices. After rigorous filtering for viable cells, 8,887 cells

were analysed for the WT and 5,309 for the KO. Cell clustering was performed using Seurat and cell types were assigned using known markers (Figure 2A) (Butler et al. 2018; Stuart et al. 2019). All expected major cell types were detected and WT and KO cells clustered together regardless of their genotype (Figure 2B).

To define TCF-4-dependent networks in commissure forming neurons, the MAST algorithm was used to determine differentially expressed genes (DEGs) between *Satb2* expressing glutamatergic WT (2,890 cells) and KO (1,328 cells) neurons (Figure 2C and Table S1) (Finak et al. 2015). Upregulated genes (97 genes) were associated with GO terms for ribosomes and gene expression (Figure 2D). GO terms for downregulated genes (131 genes) included gene enrichments for neuron development (e.g. *Bcl11a, Cux1, Dab1 and Pou3f2*) and differentiation (e.g. *Dok5, Rab3a, Sept7 and Tubb3*) as well as axon guidance (e.g. *Dcx, Nrp1, Plxna4, and Robo2*) (Figure 2D and E).

Analysis of unique molecular identifiers (UMIs), number of genes and the percentage of mitochondrial genes revealed that KO cells had in general a lower number of expressed genes and UMIs. We therefore limited the data to cells with less than 4000 UMIs, yielding 1057 WT and 1246 KO cells and re-analyzed DEG and GO term enrichment to account for potential bias introduced by differences in gene and cell number in the *Satb2* cluster. Most DEGs and GO terms remained the same indicating the biological relevance of our findings (Table S2).

Collectively, these findings molecularly confirm the anatomical observation that *Tcf4* knockout affects the expression of a gene network in *Satb2* neurons, that is involved in commissure and neuron projection development.

TCF-4 modulates the regulon activity of neurodevelopmental transcription factors

We next aimed to investigate the influence of TCF-4 on gene regulatory networks (GRNs). GRNs were calculated using the R package of SCENIC (Aibar et al. 2017). Identified regulons were binarized to generate an ON/OFF state (Figure 3A). Re-clustering displayed a partitioning of cells between the two genotypes with only marginal overlap (Figure 3A). Regulons were sorted into three categories: In the first, the regulon was primarily active in the WT. In the second, there was no differential activity between the genotypes, and in the third, the regulon was predominantly active in the KO. Differentially active regulons mostly fell into the first category [e.g.

Ctcf, *Foxg1, Smarca4* (also known as *Brg1*), *Cux1*, *Pou3f3* (also known as *Brn1*), and *Sox11]* (Figure 3B and C and Table S2). As with the DEG analysis, we repeated the analysis with the limited *Satb2* dataset and replicated these findings (Table S3). Further analysis was therefore done with the original dataset.

Examination of the differentially active regulons revealed that most regulon heads functioned as TFs. Interestingly, the respective genes were to a high extent associated with autism spectrum disorders (ASD), intellectual disability (ID) and schizophrenia [ASD: 26 genes; 32.10%; e.g. *FOXG1*; ID: 10 genes; 12.35%; e.g. *CTCF*; Schizophrenia: 13 genes; 16.05%; e.g. *SOX11* (Figure 3D)](Gregor et al. 2013; Kortum et al. 2011; Sun et al. 2020). To our surprise, these TFs generally did not belong to the bHLH TF family, which constitutes the canonical interaction partners of TCF-4 (bHLH factors: 3.70%; Other: 96.30%) (Figure 3E). In addition, the vast majority of regulators did not appear to be downstream targets of TCF-4 as they were mostly not differentially expressed in the KO (DE: 6.17%; Not DE: 93.83%) (Figure 3E). This observation raised the question of how the loss of TCF-4 impacted on regulon activity. A recent *in vitro* study suggested that TCF-4 may interact with TFs outside the bHLH family (Moen et al. 2017), leading to the hypothesis that TCF-4 interacts with the regulators and thereby modulates their activity. We thus focused on potential interactions regulating genes involved in neurogenesis or neuron differentiation. To ensure a focus on the robustly expressed regulons, we required the selected regulators to be expressed in at least one quarter of the *Satb2* expressing cells (Table S4). Five regulon heads [*Foxg1, Smarca4* (also known as *Brg1*), *Cux1*, *Pou3f3* (also known as *Brn1*), and *Sox11*] were selected for validation (Figure 3C). CUX1 and POU3F3 are specific markers for layer II/III neurons, whereas FOXG1, SMARCA4 and SOX11 are broadly expressed during neuronal differentiation (Bergsland et al. 2006; Campbell et al. 2008; Deng et al. 2015; Miyoshi and Fishell 2012; Molyneaux et al. 2007; Seo 2004). Staining of neocortical tissue at E18.5, showed that TCF-4 was co-expressed with SOX11, FOXG1, SMARCA4 and POU3F3 (Figure 3F). *In vitro* co-immunoprecipitation assays confirmed that the long TCF-4 isoform has the potential to biochemically interact with all these TFs (Figure 3G). Moreover, co-immunoprecipitation assays from E18.5 neocortex lysates validated the interaction of TCF-4 with SOX11 *in vivo* (Figure 3H).

Thus, TCF-4 has the ability to biochemically interact with a wide variety of TFs and chromatin remodelers involved in neurogenesis and neuronal differentiation and may thereby modulate their activity during commissure development.

TCF-4 and SOX11 act synergistically during commissural development

We focused our successive investigation on the interaction of TCF-4 and SOX11. SOX11 contributes to an evolutionary conserved program controlling axonal tract formation of corticospinal neurons (Shim et al. 2012). SOX11's importance for human neurodevelopment is demonstrated by its causal link to a Coffin-Siris-like syndrome (OMIM 615886), a neurodevelopmental disease characterised by microcephaly and intellectual disability (Hempel et al. 2016; Turan et al. 2019). Assessing the mRNA levels in the *Satb2* cluster, *Sox11* was found to be expressed in almost every cell, rendering it the most commonly expressed regulator examined.

To evaluate the functional interaction of TCF-4 and SOX11 *in vivo, Tcf4* and *Sox11* haploinsufficient mice were crossed to generate WT, *Tcf4, Sox11* and double *Tcf4* and *Sox11* haploinsufficient littermates. Commissural systems in P56 brains were visualized by Luxol fast blue staining. WT and *Sox11* haploinsufficient mice showed no commissural phenotype (Figure 4A). In line with a previous report, *Tcf4* haploinsufficient animals had a mildly shortened CC (data not shown) (Jung et al. 2018). This phenotype was greatly aggravated by the additional haploinsufficiency of *Sox11* as double haploinsufficient mice showed the most severe truncation of the CC with only the most rostral part of the CC remaining (agenesis of the splenium and caudal part of the body) (Figure 4A). Moreover, only a rudimentary AC (1 out of 5 animals) or a complete agenesis of the AC (4 out 5 animals) was observed in the double haploinsufficient mice (Figure 4A).

We next asked which genes may be common target genes of both TFs and thus may be involved in commissure development. Hence, we compared the predicted regulon targets of SOX11 from the GRN analysis and the list of DEGs in the *Tcf4KO*. The intersection of the datasets yielded a list of 73 genes (Figure 4B and Table S3), which similarly to the differentially active regulons were often associated with autism spectrum disorders, intellectual disability and schizophrenia [ASD: 31 genes; 42.47%; e.g. *GRIA2*; ID: 14 genes; 19.18%; e.g. *DCX*; Schizophrenia: 22 genes; 30.14%; e.g. *PLXNA2* (Figure 4C)] (Mah et al. 2006; Pilz et al. 1998; Salpietro et al. 2019). Furthermore, GO term analysis revealed an enrichment for genes involved in

axonogenesis (Figure 4D and Table S3). From these associated genes *Plxna2*, a gene involved in semaphorin plexin signalling for axon guidance (Mah et al. 2006; Mitsogiannis et al. 2017; Rohm et al. 2000) and *Dcx*, a gene essential for proper neuronal morphology, migration and axon guidance were selected for further investigation (Deuel et al. 2006; Fu et al. 2013; Karl et al. 2005; Koizumi et al. 2006). Evolutionary conserved regions upstream of or at the promotor, which contained conserved binding sites for TCF-4 and SOX11, were cloned into luciferase reporter plasmids and then transfected into HEK293T cells together with expression plasmids for *Tcf4* and *Sox11*. SOX11 alone induced robust *Dcx* and *Plxna2* reporter activity. TCF-4 alone only marginally induced *Plxna2* and *Dcx* activity but strongly potentiated SOX11 induced reporter activities (*Dcx*: SOX11 vs. TCF4+SOX11: p-value = 0.0059; TCF4 vs. TCF4+SOX11: p-value = 0.0011; *Plxna2*: SOX11 vs. TCF4+SOX11: p-value = 0.0018; TCF4 vs. TCF4+SOX11: p-value = 0.0021) (Figure 4B and C).
Collectively, these results indicate the cooperative interaction of TCF-4 and SOX11 in AC and CC formation by activating gene expression and their importance in axonogenesis and axon guidance.

Discussion

Interhemispheric connections are central for higher brain function by integrating information from both hemispheres (Constantinidis and Klingberg 2016; Hedden and Gabrieli 2004). Here, we show that *Tcf4* knockout severely disrupts cortex development, especially commissure formation. We provide scRNA-Seq and biochemical evidence that positions the bHLH transcription factor TCF-4 at the centre of a large regulatory network for forebrain commissure formation. Of particular interest is the finding that in this network TCF-4 interacts with multiple intellectual disability, autism and schizophrenia associated transcriptional regulators raising the possibility that the TCF-4 dependent regulatory network in commissure formation may be relevant for the pathogenesis of neurodevelopmental and -psychiatric disorders.
Previous analysis revealed the existence of multiple TCF-4 isoforms (Sepp et al. 2011). TCF-4A (short isoform) and TCF-4B (longest isoform) have been identified as the two main TCF-4 isoforms, yet their specific function is presently not understood. The isoforms of TCF-4 differ in their domain structure as the longest isoform contains an additional activation domain, the only nuclear localization signal and another

repressor domain. In addition, analysis of transactivation efficiency has shown that TCF-4B has a higher capacity to induce gene expression than its shorter counterparts (Sepp et al. 2011). The present *Tcf4KO* mouse model displays residual expression of a short isoform of TCF-4 (TCF-4A), yet the fact that a loss of forebrain commissures was observed, strongly suggests that the longest isoform has singular functions in commissural formation. In this regard, future studies should compare the ability of TCF-4 isoforms for interaction with the identified transcription factor network and should map the respective interaction domains in the TCF-4 protein. An alternative, however, less likely explanation, given the additional functional domains of the long TCF-4B isoform would be that commissural development is highly dependent on TCF-4 dosage irrespective of the expressed isoforms.

Callosal abnormalities have been described in patients with PTHS who carry loss-of-function mutations in the bHLH domain (Amiel et al. 2007; Jung et al. 2018; Zweier et al. 2007). Disruption of the bHLH domain results in impaired DNA-binding affecting the transcriptional function of all TCF-4 isoforms (Sepp et al. 2012). Mutations in the first seven exons of *TCF4,* which do not affect the bHLH domain and may allow for the expression of shorter isoforms with an intact bHLH domain have been found in patients with moderate ID (Bedeschi et al. 2017). The present data raise the interesting possibility that such mutations may be sufficient to disrupt the function of TCF-4 in the development of interhemispheric connectivity and it would be interesting to investigate if these patients also display abnormalities in intercortical connectivity.

In line with a previous study by Li and colleagues (Li et al. 2019), who analysed mice homozygously carrying a loss-of-function mutation affecting the bHLH domain of TCF-4, we found that loss of TCF-4 promotes the generation of SATB2+ neurons at the expense of deep layer neurons. While we have not analysed the molecular basis of these alterations, these data indicate that the loss of the commissural system in *Tcf4*KO mice is not the result of a failure to generate interhemispheric projection neurons and that TCF-4 is dispensable for the specification of SATB2+ neurons.

Dysplasia of the commissure system may not only be caused by impaired development of the respective projection neurons, but also by the failure to properly form a midline (Richards et al. 2004). In our analyses, the cellular composition of the midline appeared unaffected. At this point, we cannot fully exclude the possibility that subtle defects in midline cell composition and the erroneous display of axonal guidance cues contributed to the CC defects. The failed formation of the AC and the

hippocampal commissure, though, hints at a general defect of neurons for commissure formation as these structures do not depend on midline fusion (Raybaud 2019).

While this study was in review, Mesman and colleagues reported the agenesis of the forebrain commissure system in a different *Tcf4* knockout mouse model (Mesman et al. 2020), which underlines the importance of TCF-4 in establishing interhemispheric connectivity. In contrast to our study, Mesman and colleagues found subtle defects in midline formation (Mesman et al. 2020). These phenotypic differences may be explained by the different genetic setup of the respective *Tcf4*KO models. While the present *Tcf4*KO model allowed for the residual expression of shorter TCF-4 isoforms with a functional bHLH domain, the *Tcf4* KO strain analysed by Mesman and colleagues harboured a mutation that removed the DNA binding bHLH domain from all isoforms (Mesman et al. 2020). Hence, future studies should address to what extent different TC-F4 isoforms contribute to the development of the midline.

Bulk RNA-Sequencing analyses of the developing murine neocortex of *Tcf4*KO mice showed that TCF-4 regulates a diverse set of genes with functions in cell proliferation, neuronal differentiation, and neurotransmitter release (Li et al. 2019; Mesman et al. 2020), which reflects TCF4's pleiotropic functions in cortical development (Li et al. 2019; Mesman et al. 2020; Page et al. 2017). However, given the broad expression of TCF4 (Jung et al. 2018) and the considerable cellular diversity in the developing neocortex, bulk RNA-Sequencing data is not ideally suited to molecularly explain the complex phenotype of *Tcf4*KO mice and to identify cell-type and or stage-specific TCF-4 dependent mechanisms. In the present study, we used comparative single cell RNA-Sequencing analysis to zoom in onto the TCF-4-dependent transcriptome in *Satb2*-expressing neurons. We thereby uncovered that TCF-4 regulates genes with functions in axon guidance and neuronal and axonal development in this cell population, which provides a molecular explanation for the commissural phenotype in *Tcf4*KO mice. As the present data set contains single-cell RNA sequencing data from the developing neocortex, it provides an important resource to identify the cell type specific TCF-4 dependent transcriptome for other defined neocortical cell populations. Such analyses are expected to provide a better understanding of how TCF-4 functions as a pleiotropic regulator of cortex development.

Our approach of gene regulatory network analysis enabled us to identify how TCF-4 may affect these downstream targets. Classically, it had been assumed that TCF-4 partners with tissue specific bHLH TFs to influence transcription. Our results together with a recent *in vitro* study in mouse neuronal stem cells (Moen et al. 2017) indicate that TCF-4 also interacts with a multiplicity of TFs and chromatin remodelers outside the bHLH family to modulate their transcriptional activity. Here, we provided the first *in vitro* and *in vivo* biochemical evidence for these interactions and expanded the interactome of TCF-4 in a cell type specific manner for postmitotic intercortical projection neurons. As the scRNA data set is not restricted to intercortical projection neurons, it allows to predict cell type specific TCF-4-interactors also in other neocortical cell types, which will help to promote the understanding of how TCF-4 regulates the development of distinct cell populations.

Current evidence suggests that CC dysgenesis significantly contributes to cognitive impairment and associative dysfunction in intellectual disability, autism, and schizophrenia (Arnone et al. 2008; Badaruddin et al. 2007; Bedeschi et al. 2006; Hallak et al. 2007; Jeret et al. 1985; Paul et al. 2007; Rao et al. 2011; Siffredi et al. 2013). Intriguingly, many of the identified interactors are associated with these disorders and several of them are themselves linked to structural abnormalities of the CC (Cargnin et al. 2018; Filatova et al. 2019; Pinero et al. 2020; Pringsheim et al. 2019; Snijders Blok et al. 2019; Tzeng et al. 2014).

In-depth study of the interaction of TCF-4 with SOX11 - provided *in vivo* biochemical and functional evidence for cooperativity of neurodevelopmental disorder-linked genes in the generation of the commissural system and for the regulation of factors suggested in the pathogenesis of neuropsychiatric disease. We propose that the present data provides a new entry point towards understanding central dysregulated networks in the pathogenesis of autism and schizophrenia. Finally, we demonstrate that scRNA-Seq data can be harnessed to predict interaction partners of proteins. This powerful approach will be valuable to infer cell type specific transcription factor networks from complex tissues thereby enabling the discovery of regulatory networks in development, physiology and disease.

Material and Methods

Experimental models

All experiments were carried out in accordance with the European Communities Council Directive (86/609/EEC) and were approved by the government of Middle-Franconia. Tcf4ex4WT/lacZ mice were obtained from the Wellcome Trust Sanger Institute and previously described in Jung et al. (2018) (Alleles produced for the EUCOMM and EUCOMMTools projects by the Wellcome Trust Sanger Institute; MGI ID: 4432303). The Sox11$^{LacZ/WT}$ mice were previously described (Sock et al. 2004). Experiments were performed on male and female littermates between E16.5 and P56. For embryonic studies, mice were bred in the afternoon and vaginal post-coitum protein plug check ("Plug check") was performed the next morning. This time point was defined as E0.5. Numbers of animals used in each experiment are indicated in the figure legends.

Genotyping of the mice was done using the following primers:

Tcf4ex4WT/lacZ	fwd Mut	TCG TGG TAT CGT TAT GCG CC
	fwd WT	CCG ATG ACA GTG ATG ATG GT
	rev	AAG TTA AGC TGA AGT AAA TAC CCA CA
	lacZ fwd	ATC ACG ACG CGC TGT ATC
	lacZ rev	ACA TCG GGC AAA TAA TAT CG
Sox11$^{LacZ/WT}$	fwd	GCC CGC GCA GGA GAC CGA GC
	Rev	CTT GTA GTC GGG GTA GTC AGC C
	lacZ	CGC TCAGGT CAA ATT CAG AC

HEK 293T cells (ATCC, Wesel, Germany; CRL-3216) were in 10 cm dishes in DMEM supplemented with 10% of fetal bovine serum and 5 ml penicillin/Streptomycin at 37°C and 5% CO_2.

Experimental Design

For the single-cell RNA-Sequencing (5 WT and 4 KO samples) only samples with more than 500 cells after filtering were used to ensure a complete reproduction of cell diversity in the neocortex. Therefore, 2 samples for the WT and 2 samples for the KO

were removed. We had to exclude one WT animal that displayed lower *Tcf4* expression than the KO and also excluded one cluster that displayed a high background transcript expression of blood related genes such as Hbb-a1, Hbb-a2.

Tissue preparation and dissection

Timed pregnant mice were killed by cervical dislocation. For the E16.5, E18.5 and P0 time points, brains were dissected and fixed overnight in 4% PFA. Tails were used for genotyping. After fixation tissue was washed repeatedly with 1× PBS and transferred to 30% sucrose in 0.1 M phosphate buffer overnight for dehydration. Embryonic tissues were embedded in freezing media (Leica Biosystems, Richmond) and stored at −80°C. Adult mice were killed using CO_2 and transcardially perfused with PBS for 2 min (20 ml/min) followed by fixation with 4% paraformaldehyde (PFA) in PBS, pH 7.4, for 5 min. The brains were post-fixed overnight in 4% PFA at 4°C followed by dehydration at 4°C in 30% sucrose in 0.1M phosphate buffer.

Histology

Embryonic tissue was cut in 10 µm thin sections with a cryotom (Leica Microsystems, Wetzlar). Sections were transferred on laminated object slides, dried for 2 h at room temperature and stored at −80°C until further use. Slides were washed once for 5 min with 1x PBS. For antigen retrieval, sections were treated with 10 mM citrate buffer (pH 6) for 11 min at 720 watt in the microwave. Afterwards, half of the citrate buffer was replaced by water and the sections were incubated for another 30 min. Further steps were performed for both antigen retrieval and normal staining protocol. Slides were washed once in 1x PBS and subsequently incubated in 4% PFA for 10 min followed by two more washing steps in 1x PBS. Tissue was permeabilized for 10 min in 0.3% Triton-X/PBS and blocked with blocking solution (10% Donkey serum, 3% BSA and 0.1% Tween20 in PBS) for at least 1 h in a wet chamber at room temperature. Sections were incubated with primary antibodies [rb BRN1 (kind gift of Elisabeth Sock) 1:500); rb BRG1 (Santa Cruz, sc10768) 1:100; rb CALRETININ (Swant 7699/4) 1:500; rt CTIP2 (Abcam, 18465) 1:500; ab rb FOXG1 (Abcam, ab18259) 1:500; rb GAP43 (Abcam, ab5220) 1:500; ch GFAP (Abcam, ab4674) 1:500; ms SATB2 (Santa Cruz, sc-81376), 1:500; rat anti-SOX11 (kind gift from Johannes Glöckner) 1:500; rb TBR1 (Abcam, ab31940) 1:500; ms TCF-4 (Santa

Cruz, sc393407) 1:100] diluted in blocking solution at 4°C overnight. Slides were washed three times for 5 min with 1x0.1% Tween/PBS, incubated with secondary antibodies diluted in blocking solution for 2 h at room temperature, and washed three times with 1x PBS. Nuclei were stained with DAPI (500 pg/ml in 1x PBS) for 10 min. After additional washing with 1x PBS for 5 min, slides were mounted with 60 µl Mowiol (Sigma Aldrich Chemie GmbH Munich, Germany) and stored at 4 C.

Cell counting

Cell counting was done blind to avoid bias. Numbers were randomly assigned to slides before imaging. Genotypes were only revealed for statistical analysis. All images of the cortices were taken with the pial surface at the upper edge of the picture and the ventricular surface at the lower edge. Cells in an image were counted using ImageJ software and reported as the total numbers of cells per surface area of the VZ.

Lipophilic Tracer Analysis

For the lipophilic tracer experiment P0 brains were dissected, washed once in 1xPBS and dried on a soft tissue. 1 µl of DiI dilution [DiIC18(3), Invitrogen, Eugene, Orgeon] was pipetted on one hemisphere and the brain subsequently fixed in 4% PFA. After six weeks the tissue was transferred to 30% sucrose in 0.1 M phosphate buffer overnight for dehydration, then frozen in tissue freezing media (Leica Biosystems, Richmond) and stored at − 80 C. Brains were cut in 10 µm thin sections with a cryotom (Leica Microsystems, Wetzlar). Sections were transferred on laminated object slides and dried for 2 h at room temperature. Slides were washed three times with 1x PBS and nuclei stained with DAPI (1:10.000 in 1xPBS) for 10 min. After additional washing with 1x PBS for 5 min, slides were mounted with 60µl Mowiol (Sigma Aldrich Chemie GmbH Munich, Germany) and stored at 4°C.

Luciferase Assay

The ECR from the *Plxna2 gene* had the following positions in Mm10: chr1:194607209-194608066. The ECR was obtained by PCR from WT mouse DNA and inserted into the pTATA luciferase reporter plasmid in front of a β-globin minimal promoter. The hDCX-Promotor plasmid has been described before (Karl et al. 2005).

HEK cells were seeded in a density of 80.000 cells per well in a 24 well plate and transfected the next day. 400 ng of CAG-GFP-based expression vectors (CAG-GFP ; CAG-*Sox11*-IRES-GFP (Balta et al. 2018); CAG-TCF-4-IRES-GFP (Jung et al. 2018)) , 200 ng of luciferase reporter (hDCX-pGL3 (Karl et al. 2005) and pTataLuc-Plxna2) and 10 ng of Renilla expression plasmid per well were transfected using JETPEI (Polyplus transfection, 101-10 N) according to the manufacturers' instruction. Three wells were transfected per condition as technical replicates. After 48 h Luciferase assay was performed according to manufacturers' instruction using the Dual-Luciferase Reporter Assay System Kit (Promega).

Luxol fast blue staining

To stain for myelin with luxol fast blue (Polyscience, Hirschberg an der Bergstraße) free floating sections were washed two times with 1x PBS, mounted on coated adhesive glass slides and dried for at least 2 hours at RT. The glass slides were incubated in luxol fast blue solution at 57°C overnight and then washed one time in 95% ethanol and one time in distilled water. The staining was differentiated in lithium carbonate solution for 3 min followed by incubation in 70% ethanol till white and grey mater was distinguishable. If this takes longer than 5 min, the glass slides are washed in distilled water again and the differentiation steps are repeated until white and grey mater are distinguishable from each other. The nuclei were stained with Mayer´s hemalun solution for maximal 30 sec and excess solution was removed by rinsing with tap water. Slides were mounted with 60 µl Mowiol and stored at 4°C.

Imaging

For overview images and cell counting, fluorescence signal was detected with an AF6000 Modular Systems Leica fluorescent microscope and documented with a SPOT-CCD camera and the Leica software LAS AF (Version 2.6.0.7266; Leica Microsystems, Wetzlar Germany). For the analysis of the Luxol fast blue staining, images were obtained with a Zeiss MN Imager and x 2.5 objective lens. For co-expression analysis, fluorescence signal was detected using a Zeiss LSM 780 confocal microscope with four lasers (405, 488, 550, and 633 nm) and × 40 objective lens. Images were processed using ImageJ.

Co-Immunoprecipitation

For *in vitro* Co-Immunoprecipitation HEK 293T cells (ATCC, Wesel, Germany; CRL-3216) were seeded in a density of two million cells in 10 cm dishes in DMEM supplemented with 10% of fetal bovine serum and 5 ml penicillin/Streptomycin. At a confluency of 70-90% cells were transfected using JETPEI (Polyplus transfection, 101-10 N) with equal amounts of the expression vectors (7.5 µg/10 cm dish) of CAG-TCF-4-IRES-GFP and the predicted interaction partners [pCMV5 rBrn1(Schreiber et al. 1997) ; pBJ5-hBRG1 (pBJ5 hBRG1 was a gift from Jerry Crabtree (Addgene plasmid # 17873 ; http://n2t.net/addgene:17873 ; RRID:Addgene_17873))(Khavari et al. 1993); pXJ42-p200 CUX1 (pXJ42-p200 CUX1 was a gift from Alain Nepveu (Addgene plasmid # 100813 ; http://n2t.net/addgene:100813 ; RRID:Addgene_100813))(Wilson et al. 2009); CAG-*Foxg1*-IRES-RFP; CAG-*Sox11*-IRES-GFP(Balta et al. 2018)) according to the manufacturer instruction. After 48 h, cells were harvested in 1 ml Buffer A [10 mM Hepes, pH 7.9, 10 mM KCl, 0.1 mM EDTA, pH 8.0, 0.1 mM EGTA, pH 8.0, protease inhibitor EDTA free cocktail (Roche PVT GmbH Waiblingen, Germany) and Phosphatase Inhibitors Cocktail (Sigma Aldrich Chemie GmbH Munich, Germany)] (330µl per 10 cm dish). Three 10 cm dishes were combined for every experiment. After addition of 100 µl of 10% NP-40 and 84 µl of 5 M NaCl the solution was vortexed for 10 sec followed by 15 min of incubation on a rotating wheel at 4°C. The homogenates were centrifuged at 14000xg for 3 min. The supernatant was used directly for the co-immunoprecipitation by mixing 300 µl with 1.2 ml of TEN-Buffer [10 mM Tris, pH 7.4, 0.05 mM EDTA, 50 mM NaCl, 0.25% 10%NP40, protease inhibitor EDTA free cocktail (Roche PVT GmbH Waiblingen, Germany) and Phosphatase Inhibitors Cocktail (Sigma Aldrich Chemie GmbH Munich, Germany)] and 2 µl of ms TCF-4-antibody (Santa Cruz, sc393407), 2 µl of ms BrdU-antibody (BD Bioscience, B44) (Control for unspecific binding to mouse antibodies), or nothing to control for unspecific binding to Protein A Agarose Beads, Fast Flow (GE Healthcare Bio-Sciences AB, Uppsala, Sweden). An appropriate amount of the supernatant was kept as Input. Prepared probes were incubated on a rotating wheel at 4°C overnight. 30 µl of Protein A Agarose Beads, Fast Flow (Millipore-Merck, Darmstadt) in TEN-Buffer (1:1) were added and the samples were rotated for another 3 h at 4°C. Samples were centrifuged for 5 min at

1200xg and the supernatant was discarded. Beads were then washed three times with 500 µl of TEN-Buffer and frozen at -80°C. For Western Blot analysis 30 µl of 3xLaemmli buffer was added to the beads and incubated at 95°C for 5 min. 30 µl of the samples were loaded on 10% 1,5 mm SDS gels.

For *in vivo* Co-Immunoprecipitation, neocortices of E18.5 WT embryos were dissected and either used directly or stored at -80°C until further use. Two cortices were merged and homogenized in 1 ml of Buffer A. Samples were treated as described above. Antibodies used were rb SOX11-antibody (Abcam, ab134107) and rb EPHA3-antibody (Abcam, ab110465). For Western Blot analysis 50 µl of 3xLaemmli buffer was added to the beads and incubated by 95°C for 5 min. 50 µl of the samples were loaded on 10% 1,5 mm SDS gels.

Western Blot

Protein extracted from E18.5 WT or KO cortices were obtained by homogenizing the tissue in RIPA buffer [50 mM Tris-HCl, pH 8.0, 150 mM NaCl, 1% Nonidet P-40, 0.5% Na-deoxycholate, 0.1% SDS, 2 mM EDTA, protease inhibitor EDTA free cocktail (Roche PVT GmbH Waiblingen, Germany) and Phosphatase Inhibitors Cocktail (Sigma Aldrich Chemie GmbH Munich, Germany)] followed by incubation for 30 min on ice. The post-nuclear supernatant of the lysate was obtained by centrifugation at 2000xg for 10 min at 4°C. Protein content was measured using the Pierce BCA protein assay (Thermo Scientific, Warrington, UK). For Western Blot analysis 30 µg of protein were loaded on a 10% 1mm SDS-PAGE gel. Gels underwent wet transfer onto a nitrocellulose membrane. Membranes were blocked in PBS with 0.1% Tween 20 (PBS-T). Incubation with primary antibodies [rb TCF-4 (Abcam; ab130014) 1:500] diluted in 5% BSA in PBS-T was performed overnight at 4°C and was followed by three times washing with PBS-T. Secondary antibodies were diluted in PBST and incubated with the membranes for at least 1 h at room temperature followed by washing with PBS-T. Membranes were treated with Clarity Western Enhanced Chemiluminescence Substrate (Bio-Rad) and visualized with Fusion-SL (PeqLab). Images were processed via Fusion (PeqLab).

Single-cell RNA sequencing and analysis

Single-Cell Isolation of E18.5 cortex tissue

Neocortices of E18.5 embryos were dissected under a binocular. Each cortex was incubated in 150 µl of Ovomucoid-Mix [1.15 mg/ml Trypsin-Inhibitor (Sigma Aldrich Chemie GmbH Munich, Germany), 0.53 mg/ml BSA, 400 ng/ml DNase I Type IV (Roche PVT GmbH Waiblingen, Germany) in L15 medium (Gibco)] and carefully cut into small pieces. After addition of 150 µl of Papain-Mix (30 U/ml Papain (Sigma Aldrich Chemie GmbH Munich, Germany), 0.24 mg/ml Cysteine (Sigma Aldrich Chemie GmbH Munich, Germany), 40 µg/ml DNase I Type IV (Roche PVT GmbH Waiblingen, Germany)) samples were incubated for 15-20 min at 37°C. To dissociate the cells. 300 µl of Ovomucoid were added followed by a 5 min incubation at room temperature. The tissue was then triturated with fire-polished glass pipettes and transferred to 10 ml of L15 medium. To obtain the cells, the solution was centrifuged for 5 min at 90xg and about 9.5 ml of the supernatant was discarded. Cells were resuspended in the remaining media and strained through a cell strainer (Mesh size: 40 µm) to remove clumps. Cell density was determined using a Neubauer chamber. Libraries were prepared using the Chromium Controller and the Chromium Single Cell 3' Reagent Kit v2 (10X Genomics, Pleasanton, CA). Single cell suspensions were diluted in nuclease-free water according to manufacturer instructions to obtain a targeted cell count of 5000. cDNA synthesis, barcoding, and library preparation were then carried out according to the manufacturers' instructions. The libraries were sequenced on an Illumina HiSeq 2500 (Illumina, San Diego) with a read length of 26 bp for read 1 (cell barcode and unique molecule identifier (UMI)), 8 bp i7 index read (sample barcode), and 98 bp for read 2 (actual RNA read). Reads were first sequenced in the rapid run mode, allowing for fine-tuning of sample ratios in the following high-output run. Combining the data from both flow cells yielded approximately 200 M reads per mouse.

Data Processing for scRNA-seq Analysis Using Cell Ranger and Seurat

The reads were de-multiplexed using Cell Ranger (version 2.1.1, 10X Genomics) mkfastq and read quality was assessed by FastQC (version 0.11.8, Babraham

bioinformatics). For mapping the reads to the mm10 genome (10X Reference 2.1.0, GRCm38, Ensembl 84) and to identify single cells the standard Cell Ranger workflow was used. Common quality control measures for scRNA-seq (gene count per cell, UMI count per cell, percent of mitochondrial transcripts) were calculated using the Seurat R package (version 2.3.4) (Butler et al. 2018; Satija et al. 2015). The analyses were performed for genotypes and for each mouse individually. Quality control thresholds were set to 1,000-5,000 genes per cells, 1800-10000 UMIs and <6% of mitochondrial transcripts. Only samples with more than 500 cells after filtering were used to ensure a complete reproduction of cell diversity in the neocortex. 3 samples for WT and 2 samples for KO were used for further analysis. We had to exclude one WT animal that displayed lower *Tcf4* expression than the KO and we also excluded cells that displayed a high background transcript expression of blood related genes such as Hbb-a1, Hbb-a2.

scRNA-Seq clustering and differential gene expression analysis using Seurat

Clustering of the cells was performed using the Seurat packages for R following the vignettes of the authors (Butler et al. 2018; Stuart et al. 2019). Cluster identity was defined using known marker expression for the different cell types. To extract SATB2 expressing glutamatergic cells, the data was subset by accepting only cells belonging to the intermediate progenitor, newborn neuron, deep layer and upper layer clusters with counts for SATB2 above 0. Differentially expressed genes between the two genotypes were determined using the MAST algorithm as implemented implementation in Seurat (Finak et al. 2015). GO-terms were identified with the Panther online tool (GO- Slim biological process and GO biological process complete) (http://www.pantherdb.org) (Mi et al. 2019).

Gene regulatory network analysis by SCENIC

Assessment of gene regulatory networks (GRNs) was performed using the R package SCENIC (version 2) (Aibar et al. 2017). Only genes expressed in at least three cells were considered for analysis. The analysis was performed according to the packages vignettes. After gene regulatory networks defined, the networks were binarized. To that end a threshold was set at the mean of the area under the curve. In cells below the threshold the GRN was considered not active (OFF) whereas in

cells above it was considered active (ON). As cells clustered apart according to the genotype, a list of GRNs was identified which where only active in one genotype. It was hypothesised that TCF-4 interacts with the heads of the GRNs and modulates their activity. To obtain a manageable list of candidate genes which might interact with TCF-4 the list of GRNs heads were analysed using the Panther online tool (Mi et al. 2019). Only genes associated with the GO terms neurogenesis/neuron differentiation and with at least an expression in 1/4 of the cells in the SATB2 cluster were chosen for validation. Common targets of TCF-4 and SOX11 were found by intersecting the list of DEGs from the *Satb2* cluster with the predicted targets of the Sox11 regulon. Disease association was determined by querying the list of differentially active regulons and common targets of TCF-4 and Sox11 in the DisGeNET database (https://disgenet.org)(Pinero et al. 2020).

Statistical analysis

To determine statistical significance Mann-Whitney-U test was performed using the ggplot2 implementation of R (*, P ≤0.05; **, P ≤0.01, ***, P ≤0.001) if not otherwise indicated. n is indicated in the figure legends. Data is depicted as mean ± SD.

To determine whether differences in luciferase activities (Figure 4B and C) were statistically significant, a two-tailed student´s t-test was performed using the ggplot2 implementation of R (*, P ≤0.05; **, P ≤0.01, ***, P ≤0.001). Data is depicted as mean ± SD. Results from independent transfections were treated as biological replicates.

Data and code availability

The accession number for the single-cell RNA Sequencing of E18.5 neocortices is GEO: GSE147247.

Acknowledgments

We thank Silvia Cappello, Michael Wegner and all members of the Institutes of Human Genetics and Biochemistry for helpful discussions.

This work was supported by the Deutsche Forschungsgemeinschaft (DFG, German Research Foundation) [Grant numbers 270949263/ GRK2162 and LI 858/ 9-1], by the Interdisciplinary Centre for Clinical Research Erlangen [Grant number E16 to D.C.L. and A.R.], and the Bavarian Research Network “ForINTER” to D.C.L..

M.T.W. is member of the research training group 2162 “Neurodevelopment and Vulnerability of the Central Nervous System” of the Deutsche Forschungsgemeinschaft (DFG GRK2162/1).

Author contributions

Conceptualization, M.-T.W., D.C.L., A.R; Investigation, M.-T.W., P.K., A.B.E., Formal analysis, M.-T.W., P.K., A.B.E., D.C.L., A.R; Resources and Funding acquisition, D.C.L., A.R; Reagents, E.S.; Writing-Original draft, M.-T.W., D.C.L., A.R.; Writing-Review and Editing, M.-T.W., D.C.L., A.R.; Supervision: D.C.L., A.R.

Declaration of Interests

The authors declare no competing interests.

References

Aibar S, Gonzalez-Blas CB, Moerman T, Huynh-Thu VA, Imrichova H, Hulselmans G, Rambow F, Marine JC, Geurts P, Aerts J, van den Oord J, Atak ZK, Wouters J, Aerts S (2017) SCENIC: single-cell regulatory network inference and clustering. Nat Methods 14: 1083-1086. doi: 10.1038/nmeth.4463

Alcamo EA, Chirivella L, Dautzenberg M, Dobreva G, Farinas I, Grosschedl R, McConnell SK (2008) Satb2 regulates callosal projection neuron identity in the developing cerebral cortex. Neuron 57: 364-77. doi: 10.1016/j.neuron.2007.12.012

Amiel J, Rio M, de Pontual L, Redon R, Malan V, Boddaert N, Plouin P, Carter NP, Lyonnet S, Munnich A, Colleaux L (2007) Mutations in TCF4, encoding a class I basic helix-loop-helix transcription factor, are responsible for Pitt-Hopkins syndrome, a severe epileptic encephalopathy associated with autonomic dysfunction. Am J Hum Genet 80: 988-93. doi: 10.1086/515582

Arnone D, McIntosh AM, Tan GM, Ebmeier KP (2008) Meta-analysis of magnetic resonance imaging studies of the corpus callosum in schizophrenia. Schizophr Res 101: 124-32. doi: 10.1016/j.schres.2008.01.005

Badaruddin DH, Andrews GL, Bolte S, Schilmoeller KJ, Schilmoeller G, Paul LK, Brown WS (2007) Social and behavioral problems of children with agenesis of the corpus callosum. Child Psychiatry Hum Dev 38: 287-302. doi: 10.1007/s10578-007-0065-6

Balta EA, Schaffner I, Wittmann MT, Sock E, von Zweydorf F, von Wittgenstein J, Steib K, Heim B, Kremmer E, Haberle BM, Ueffing M, Lie DC, Gloeckner CJ (2018) Phosphorylation of the neurogenic transcription factor SOX11 on serine 133 modulates neuronal morphogenesis. Sci Rep 8: 16196. doi: 10.1038/s41598-018-34480-x

Bedeschi MF, Bonaglia MC, Grasso R, Pellegri A, Garghentino RR, Battaglia MA, Panarisi AM, Di Rocco M, Balottin U, Bresolin N, Bassi MT, Borgatti R (2006)

665 Agenesis of the corpus callosum: clinical and genetic study in 63 young patients.
666 Pediatr Neurol 34: 186-93. doi: 10.1016/j.pediatrneurol.2005.08.008

667 Bedeschi MF, Marangi G, Calvello MR, Ricciardi S, Leone FPC, Baccarin M,
668 Guerneri S, Orteschi D, Murdolo M, Lattante S, Frangella S, Keena B, Harr MH,
669 Zackai E, Zollino M (2017) Impairment of different protein domains causes variable
670 clinical presentation within Pitt-Hopkins syndrome and suggests intragenic molecular
671 syndromology of TCF4. Eur J Med Genet 60: 565-571. doi:
672 10.1016/j.ejmg.2017.08.004

673 Bergsland M, Werme M, Malewicz M, Perlmann T, Muhr J (2006) The establishment
674 of neuronal properties is controlled by Sox4 and Sox11. Genes Dev 20: 3475-86. doi:
675 10.1101/gad.403406

676 Bertrand N, Castro DS, Guillemot F (2002) Proneural genes and the specification of
677 neural cell types. Nat Rev Neurosci 3: 517-30. doi: 10.1038/nrn874

678 Britanova O, de Juan Romero C, Cheung A, Kwan KY, Schwark M, Gyorgy A, Vogel
679 T, Akopov S, Mitkovski M, Agoston D, Sestan N, Molnar Z, Tarabykin V (2008) Satb2
680 is a postmitotic determinant for upper-layer neuron specification in the neocortex.
681 Neuron 57: 378-92. doi: 10.1016/j.neuron.2007.12.028

682 Butler A, Hoffman P, Smibert P, Papalexi E, Satija R (2018) Integrating single-cell
683 transcriptomic data across different conditions, technologies, and species. Nat
684 Biotechnol. doi: 10.1038/nbt.4096

685 Campbell CE, Piper M, Plachez C, Yeh YT, Baizer JS, Osinski JM, Litwack ED,
686 Richards LJ, Gronostajski RM (2008) The transcription factor Nfix is essential for
687 normal brain development. BMC Dev Biol 8: 52. doi: 10.1186/1471-213X-8-52

688 Cargnin F, Kwon JS, Katzman S, Chen B, Lee JW, Lee SK (2018) FOXG1
689 Orchestrates Neocortical Organization and Cortico-Cortical Connections. Neuron
690 100: 1083-1096 e5. doi: 10.1016/j.neuron.2018.10.016

691 Constantinidis C, Klingberg T (2016) The neuroscience of working memory capacity
692 and training. Nat Rev Neurosci 17: 438-49. doi: 10.1038/nrn.2016.43

693 De Rubeis S, He X, Goldberg AP, Poultney CS, Samocha K, Cicek AE, Kou Y, Liu L,
694 Fromer M, Walker S, Singh T, Klei L, Kosmicki J, Shih-Chen F, Aleksic B, Biscaldi M,
695 Bolton PF, Brownfeld JM, Cai J, Campbell NG, Carracedo A, Chahrour MH,
696 Chiocchetti AG, Coon H, Crawford EL, Curran SR, Dawson G, Duketis E, Fernandez
697 BA, Gallagher L, Geller E, Guter SJ, Hill RS, Ionita-Laza J, Jimenz Gonzalez P,
698 Kilpinen H, Klauck SM, Kolevzon A, Lee I, Lei I, Lei J, Lehtimaki T, Lin CF, Ma'ayan
699 A, Marshall CR, McInnes AL, Neale B, Owen MJ, Ozaki N, Parellada M, Parr JR,
700 Purcell S, Puura K, Rajagopalan D, Rehnstrom K, Reichenberg A, Sabo A, Sachse
701 M, Sanders SJ, Schafer C, Schulte-Ruther M, Skuse D, Stevens C, Szatmari P,
702 Tammimies K, Valladares O, Voran A, Li-San W, Weiss LA, Willsey AJ, Yu TW, Yuen
703 RK, Study DDD, Homozygosity Mapping Collaborative for A, Consortium UK, Cook
704 EH, Freitag CM, Gill M, Hultman CM, Lehner T, Palotie A, Schellenberg GD, Sklar P,
705 State MW, Sutcliffe JS, Walsh CA, Scherer SW, Zwick ME, Barett JC, Cutler DJ,
706 Roeder K, Devlin B, Daly MJ, Buxbaum JD (2014) Synaptic, transcriptional and
707 chromatin genes disrupted in autism. Nature 515: 209-15. doi: 10.1038/nature13772

708 Deng L, Li G, Rao B, Li H (2015) Central nervous system-specific knockout of Brg1
709 causes growth retardation and neuronal degeneration. Brain Research 1622: 186-
710 195. doi: 10.1016/j.brainres.2015.06.027

711 Deuel TA, Liu JS, Corbo JC, Yoo SY, Rorke-Adams LB, Walsh CA (2006) Genetic
712 interactions between doublecortin and doublecortin-like kinase in neuronal migration
713 and axon outgrowth. Neuron 49: 41-53. doi: 10.1016/j.neuron.2005.10.038

714 Edwards TJ, Sherr EH, Barkovich AJ, Richards LJ (2014) Clinical, genetic and
715 imaging findings identify new causes for corpus callosum development syndromes.
716 Brain 137: 1579-613. doi: 10.1093/brain/awt358

717 Filatova A, Rey LK, Lechler MB, Schaper J, Hempel M, Posmyk R, Szczaluba K,
718 Santen GWE, Wieczorek D, Nuber UA (2019) Mutations in SMARCB1 and in other
719 Coffin-Siris syndrome genes lead to various brain midline defects. Nat Commun 10:
720 2966. doi: 10.1038/s41467-019-10849-y

721 Finak G, McDavid A, Yajima M, Deng J, Gersuk V, Shalek AK, Slichter CK, Miller
722 HW, McElrath MJ, Prlic M, Linsley PS, Gottardo R (2015) MAST: a flexible statistical
723 framework for assessing transcriptional changes and characterizing heterogeneity in
724 single-cell RNA sequencing data. Genome Biol 16: 278. doi: 10.1186/s13059-015-
725 0844-5

726 Fu X, Brown KJ, Yap CC, Winckler B, Jaiswal JK, Liu JS (2013) Doublecortin (Dcx)
727 family proteins regulate filamentous actin structure in developing neurons. J Neurosci
728 33: 709-21. doi: 10.1523/JNEUROSCI.4603-12.2013

729 Gregor A, Oti M, Kouwenhoven EN, Hoyer J, Sticht H, Ekici AB, Kjaergaard S, Rauch
730 A, Stunnenberg HG, Uebe S, Vasileiou G, Reis A, Zhou H, Zweier C (2013) De novo
731 mutations in the genome organizer CTCF cause intellectual disability. Am J Hum
732 Genet 93: 124-31. doi: 10.1016/j.ajhg.2013.05.007

733 Hallak JE, Crippa JA, Pinto JP, Machado de Sousa JP, Trzesniak C, Dursun SM,
734 McGuire P, Deakin JF, Zuardi AW (2007) Total agenesis of the corpus callosum in a
735 patient with childhood-onset schizophrenia. Arq Neuropsiquiatr 65: 1216-9. doi:
736 10.1590/s0004-282x2007000700024

737 Hedden T, Gabrieli JD (2004) Insights into the ageing mind: a view from cognitive
738 neuroscience. Nat Rev Neurosci 5: 87-96. doi: 10.1038/nrn1323

739 Hempel A, Pagnamenta AT, Blyth M, Mansour S, McConnell V, Kou I, Ikegawa S,
740 Tsurusaki Y, Matsumoto N, Lo-Castro A, Plessis G, Albrecht B, Battaglia A, Taylor
741 JC, Howard MF, Keays D, Sohal AS, collaboration DDD, Kuhl SJ, Kini U, McNeill A
742 (2016) Deletions and de novo mutations of SOX11 are associated with a
743 neurodevelopmental disorder with features of Coffin-Siris syndrome. J Med Genet 53:
744 152-62. doi: 10.1136/jmedgenet-2015-103393

745 Jeret JS, Serur D, Wisniewski K, Fisch C (1985) Frequency of agenesis of the corpus
746 callosum in the developmentally disabled population as determined by computerized
747 tomography. Pediatr Neurosci 12: 101-3. doi: 10.1159/000120229

748 Jung M, Haberle BM, Tschaikowsky T, Wittmann MT, Balta EA, Stadler VC, Zweier
749 C, Dorfler A, Gloeckner CJ, Lie DC (2018) Analysis of the expression pattern of the
750 schizophrenia-risk and intellectual disability gene TCF4 in the developing and adult
751 brain suggests a role in development and plasticity of cortical and hippocampal
752 neurons. Mol Autism 9: 20. doi: 10.1186/s13229-018-0200-1

753 Karl C, Couillard-Despres S, Prang P, Munding M, Kilb W, Brigadski T, Plotz S,
754 Mages W, Luhmann H, Winkler J, Bogdahn U, Aigner L (2005) Neuronal precursor-
755 specific activity of a human doublecortin regulatory sequence. J Neurochem 92: 264-
756 82. doi: 10.1111/j.1471-4159.2004.02879.x

Khavari PA, Peterson CL, Tamkun JW, Mendel DB, Crabtree GR (1993) BRG1 contains a conserved domain of the SWI2/SNF2 family necessary for normal mitotic growth and transcription. Nature 366: 170-4. doi: 10.1038/366170a0

Koizumi H, Tanaka T, Gleeson JG (2006) Doublecortin-like kinase functions with doublecortin to mediate fiber tract decussation and neuronal migration. Neuron 49: 55-66. doi: 10.1016/j.neuron.2005.10.040

Kortum F, Das S, Flindt M, Morris-Rosendahl DJ, Stefanova I, Goldstein A, Horn D, Klopocki E, Kluger G, Martin P, Rauch A, Roumer A, Saitta S, Walsh LE, Wieczorek D, Uyanik G, Kutsche K, Dobyns WB (2011) The core FOXG1 syndrome phenotype consists of postnatal microcephaly, severe mental retardation, absent language, dyskinesia, and corpus callosum hypogenesis. J Med Genet 48: 396-406. doi: 10.1136/jmg.2010.087528

Li H, Zhu Y, Morozov YM, Chen X, Page SC, Rannals MD, Maher BJ, Rakic P (2019) Disruption of TCF4 regulatory networks leads to abnormal cortical development and mental disabilities. Mol Psychiatry. doi: 10.1038/s41380-019-0353-0

Lindwall C, Fothergill T, Richards LJ (2007) Commissure formation in the mammalian forebrain. Curr Opin Neurobiol 17: 3-14. doi: 10.1016/j.conb.2007.01.008

Mah S, Nelson MR, Delisi LE, Reneland RH, Markward N, James MR, Nyholt DR, Hayward N, Handoko H, Mowry B, Kammerer S, Braun A (2006) Identification of the semaphorin receptor PLXNA2 as a candidate for susceptibility to schizophrenia. Mol Psychiatry 11: 471-8. doi: 10.1038/sj.mp.4001785

Massari ME, Murre C (2000) Helix-loop-helix proteins: regulators of transcription in eucaryotic organisms. Mol Cell Biol 20: 429-40.

Mesman S, Bakker R, Smidt MP (2020) Tcf4 encodes correct brain development during embryogenesis. Mol Cell Neurosci: 103502. doi: 10.1016/j.mcn.2020.103502

Mi H, Muruganujan A, Huang X, Ebert D, Mills C, Guo X, Thomas PD (2019) Protocol Update for large-scale genome and gene function analysis with the PANTHER classification system (v.14.0). Nat Protoc 14: 703-721. doi: 10.1038/s41596-019-0128-8

Mitsogiannis MD, Little GE, Mitchell KJ (2017) Semaphorin-Plexin signaling influences early ventral telencephalic development and thalamocortical axon guidance. Neural Dev 12: 6. doi: 10.1186/s13064-017-0083-4

Miyoshi G, Fishell G (2012) Dynamic FoxG1 expression coordinates the integration of multipolar pyramidal neuron precursors into the cortical plate. Neuron 74: 1045-58. doi: 10.1016/j.neuron.2012.04.025

Moen MJ, Adams HH, Brandsma JH, Dekkers DH, Akinci U, Karkampouna S, Quevedo M, Kockx CE, Ozgur Z, van IWF, Demmers J, Poot RA (2017) An interaction network of mental disorder proteins in neural stem cells. Transl Psychiatry 7: e1082. doi: 10.1038/tp.2017.52

Molyneaux BJ, Arlotta P, Menezes JR, Macklis JD (2007) Neuronal subtype specification in the cerebral cortex. Nat Rev Neurosci 8: 427-37. doi: 10.1038/nrn2151

Navarrete K, Pedroso I, De Jong S, Stefansson H, Steinberg S, Stefansson K, Ophoff RA, Schalkwyk LC, Collier DA (2013) TCF4 (e2-2; ITF2): a schizophrenia-associated

gene with pleiotropic effects on human disease. Am J Med Genet B Neuropsychiatr Genet 162B: 1-16. doi: 10.1002/ajmg.b.32109

Page SC, Hamersky GR, Gallo RA, Rannals MD, Calcaterra NE, Campbell MN, Mayfield B, Briley A, Phan BN, Jaffe AE, Maher BJ (2017) The schizophrenia- and autism-associated gene, transcription factor 4 regulates the columnar distribution of layer 2/3 prefrontal pyramidal neurons in an activity-dependent manner. Mol Psychiatry. doi: 10.1038/mp.2017.37

Paul LK, Brown WS, Adolphs R, Tyszka JM, Richards LJ, Mukherjee P, Sherr EH (2007) Agenesis of the corpus callosum: genetic, developmental and functional aspects of connectivity. Nat Rev Neurosci 8: 287-99. doi: 10.1038/nrn2107

Pilz DT, Matsumoto N, Minnerath S, Mills P, Gleeson JG, Allen KM, Walsh CA, Barkovich AJ, Dobyns WB, Ledbetter DH, Ross ME (1998) LIS1 and XLIS (DCX) mutations cause most classical lissencephaly, but different patterns of malformation. Hum Mol Genet 7: 2029-37. doi: 10.1093/hmg/7.13.2029

Pinero J, Ramirez-Anguita JM, Sauch-Pitarch J, Ronzano F, Centeno E, Sanz F, Furlong LI (2020) The DisGeNET knowledge platform for disease genomics: 2019 update. Nucleic Acids Res 48: D845-D855. doi: 10.1093/nar/gkz1021

Pringsheim M, Mitter D, Schroder S, Warthemann R, Plumacher K, Kluger G, Baethmann M, Bast T, Braun S, Buttel HM, Conover E, Courage C, Datta AN, Eger A, Grebe TA, Hasse-Wittmer A, Heruth M, Hoft K, Kaindl AM, Karch S, Kautzky T, Korenke GC, Kruse B, Lutz RE, Omran H, Patzer S, Philippi H, Ramsey K, Rating T, Riess A, Schimmel M, Westman R, Zech FM, Zirn B, Ulmke PA, Sokpor G, Tuoc T, Leha A, Staudt M, Brockmann K (2019) Structural brain anomalies in patients with FOXG1 syndrome and in Foxg1+/- mice. Ann Clin Transl Neurol 6: 655-668. doi: 10.1002/acn3.735

Rao NP, Venkatasubramanian G, Arasappa R, Gangadhar BN (2011) Relationship between corpus callosum abnormalities and schneiderian first-rank symptoms in antipsychotic-naive schizophrenia patients. J Neuropsychiatry Clin Neurosci 23: 155-62. doi: 10.1176/appi.neuropsych.23.2.155

10.1176/jnp.23.2.jnp155

Raybaud C (2019) Corpus Callosum: Molecular Pathways in Mice and Human Dysgeneses. Neuroimaging Clin N Am 29: 445-459. doi: 10.1016/j.nic.2019.03.006

Richards LJ, Plachez C, Ren T (2004) Mechanisms regulating the development of the corpus callosum and its agenesis in mouse and human. Clin Genet 66: 276-89. doi: 10.1111/j.1399-0004.2004.00354.x

Rohm B, Ottemeyer A, Lohrum M, Puschel AW (2000) Plexin/neuropilin complexes mediate repulsion by the axonal guidance signal semaphorin 3A. Mech Dev 93: 95-104. doi: 10.1016/s0925-4773(00)00269-0

Salpietro V, Dixon CL, Guo H, Bello OD, Vandrovcova J, Efthymiou S, Maroofian R, Heimer G, Burglen L, Valence S, Torti E, Hacke M, Rankin J, Tariq H, Colin E, Procaccio V, Striano P, Mankad K, Lieb A, Chen S, Pisani L, Bettencourt C, Mannikko R, Manole A, Brusco A, Grosso E, Ferrero GB, Armstrong-Moron J, Gueden S, Bar-Yosef O, Tzadok M, Monaghan KG, Santiago-Sim T, Person RE, Cho MT, Willaert R, Yoo Y, Chae JH, Quan Y, Wu H, Wang T, Bernier RA, Xia K, Blesson A, Jain M, Motazacker MM, Jaeger B, Schneider AL, Boysen K, Muir AM, Myers CT, Gavrilova RH, Gunderson L, Schultz-Rogers L, Klee EW, Dyment D, Osmond M,

847 Parellada M, Llorente C, Gonzalez-Penas J, Carracedo A, Van Haeringen A,
848 Ruivenkamp C, Nava C, Heron D, Nardello R, Iacomino M, Minetti C, Skabar A,
849 Fabretto A, Group SS, Raspall-Chaure M, Chez M, Tsai A, Fassi E, Shinawi M,
850 Constantino JN, De Zorzi R, Fortuna S, Kok F, Keren B, Bonneau D, Choi M,
851 Benzeev B, Zara F, Mefford HC, Scheffer IE, Clayton-Smith J, Macaya A, Rothman
852 JE, Eichler EE, Kullmann DM, Houlden H (2019) AMPA receptor GluA2 subunit
853 defects are a cause of neurodevelopmental disorders. Nat Commun 10: 3094. doi:
854 10.1038/s41467-019-10910-w

855 Satija R, Farrell JA, Gennert D, Schier AF, Regev A (2015) Spatial reconstruction of
856 single-cell gene expression data. Nat Biotechnol 33: 495-502. doi: 10.1038/nbt.3192

857 Schizophrenia Psychiatric Genome-Wide Association Study C (2011) Genome-wide
858 association study identifies five new schizophrenia loci. Nat Genet 43: 969-76. doi:
859 10.1038/ng.940

860 Schizophrenia Working Group of the Psychiatric Genomics C (2014) Biological
861 insights from 108 schizophrenia-associated genetic loci. Nature 511: 421-7. doi:
862 10.1038/nature13595

863 Schreiber J, Enderich J, Sock E, Schmidt C, Richter-Landsberg C, Wegner M (1997)
864 Redundancy of class III POU proteins in the oligodendrocyte lineage. J Biol Chem
865 272: 32286-93. doi: 10.1074/jbc.272.51.32286

866 Seo S (2004) The SWI/SNF chromatin remodeling protein Brg1 is required for
867 vertebrate neurogenesis and mediates transactivation of Ngn and NeuroD.
868 Development 132: 105-115. doi: 10.1242/dev.01548

869 Sepp M, Kannike K, Eesmaa A, Urb M, Timmusk T (2011) Functional diversity of
870 human basic helix-loop-helix transcription factor TCF4 isoforms generated by
871 alternative 5' exon usage and splicing. PLoS One 6: e22138. doi:
872 10.1371/journal.pone.0022138

873 Sepp M, Pruunsild P, Timmusk T (2012) Pitt-Hopkins syndrome-associated
874 mutations in TCF4 lead to variable impairment of the transcription factor function
875 ranging from hypomorphic to dominant-negative effects. Hum Mol Genet 21: 2873-
876 88. doi: 10.1093/hmg/dds112

877 Shim S, Kwan KY, Li M, Lefebvre V, Sestan N (2012) Cis-regulatory control of
878 corticospinal system development and evolution. Nature 486: 74-9. doi:
879 10.1038/nature11094

880 Siffredi V, Anderson V, Leventer RJ, Spencer-Smith MM (2013) Neuropsychological
881 profile of agenesis of the corpus callosum: a systematic review. Dev Neuropsychol
882 38: 36-57. doi: 10.1080/87565641.2012.721421

883 Snijders Blok L, Kleefstra T, Venselaar H, Maas S, Kroes HY, Lachmeijer AMA, van
884 Gassen KLI, Firth HV, Tomkins S, Bodek S, Study DDD, Ounap K, Wojcik MH,
885 Cunniff C, Bergstrom K, Powis Z, Tang S, Shinde DN, Au C, Iglesias AD, Izumi K,
886 Leonard J, Abou Tayoun A, Baker SW, Tartaglia M, Niceta M, Dentici ML, Okamoto
887 N, Miyake N, Matsumoto N, Vitobello A, Faivre L, Philippe C, Gilissen C, Wiel L,
888 Pfundt R, Deriziotis P, Brunner HG, Fisher SE (2019) De Novo Variants Disturbing
889 the Transactivation Capacity of POU3F3 Cause a Characteristic Neurodevelopmental
890 Disorder. Am J Hum Genet 105: 403-412. doi: 10.1016/j.ajhg.2019.06.007

891 Sock E, Rettig SD, Enderich J, Bosl MR, Tamm ER, Wegner M (2004) Gene
892 targeting reveals a widespread role for the high-mobility-group transcription factor

Sox11 in tissue remodeling. Mol Cell Biol 24: 6635-44. doi: 10.1128/MCB.24.15.6635-6644.2004

Stefansson H, Ophoff RA, Steinberg S, Andreassen OA, Cichon S, Rujescu D, Werge T, Pietilainen OP, Mors O, Mortensen PB, Sigurdsson E, Gustafsson O, Nyegaard M, Tuulio-Henriksson A, Ingason A, Hansen T, Suvisaari J, Lonnqvist J, Paunio T, Borglum AD, Hartmann A, Fink-Jensen A, Nordentoft M, Hougaard D, Norgaard-Pedersen B, Bottcher Y, Olesen J, Breuer R, Moller HJ, Giegling I, Rasmussen HB, Timm S, Mattheisen M, Bitter I, Rethelyi JM, Magnusdottir BB, Sigmundsson T, Olason P, Masson G, Gulcher JR, Haraldsson M, Fossdal R, Thorgeirsson TE, Thorsteinsdottir U, Ruggeri M, Tosato S, Franke B, Strengman E, Kiemeney LA, Genetic R, Outcome in P, Melle I, Djurovic S, Abramova L, Kaleda V, Sanjuan J, de Frutos R, Bramon E, Vassos E, Fraser G, Ettinger U, Picchioni M, Walker N, Toulopoulou T, Need AC, Ge D, Yoon JL, Shianna KV, Freimer NB, Cantor RM, Murray R, Kong A, Golimbet V, Carracedo A, Arango C, Costas J, Jonsson EG, Terenius L, Agartz I, Petursson H, Nothen MM, Rietschel M, Matthews PM, Muglia P, Peltonen L, St Clair D, Goldstein DB, Stefansson K, Collier DA (2009) Common variants conferring risk of schizophrenia. Nature 460: 744-7. doi: 10.1038/nature08186

Steinberg S, de Jong S, Irish Schizophrenia Genomics C, Andreassen OA, Werge T, Borglum AD, Mors O, Mortensen PB, Gustafsson O, Costas J, Pietilainen OP, Demontis D, Papiol S, Huttenlocher J, Mattheisen M, Breuer R, Vassos E, Giegling I, Fraser G, Walker N, Tuulio-Henriksson A, Suvisaari J, Lonnqvist J, Paunio T, Agartz I, Melle I, Djurovic S, Strengman E, Group, Jurgens G, Glenthoj B, Terenius L, Hougaard DM, Orntoft T, Wiuf C, Didriksen M, Hollegaard MV, Nordentoft M, van Winkel R, Kenis G, Abramova L, Kaleda V, Arrojo M, Sanjuan J, Arango C, Sperling S, Rossner M, Ribolsi M, Magni V, Siracusano A, Christiansen C, Kiemeney LA, Veldink J, van den Berg L, Ingason A, Muglia P, Murray R, Nothen MM, Sigurdsson E, Petursson H, Thorsteinsdottir U, Kong A, Rubino IA, De Hert M, Rethelyi JM, Bitter I, Jonsson EG, Golimbet V, Carracedo A, Ehrenreich H, Craddock N, Owen MJ, O'Donovan MC, Wellcome Trust Case Control C, Ruggeri M, Tosato S, Peltonen L, Ophoff RA, Collier DA, St Clair D, Rietschel M, Cichon S, Stefansson H, Rujescu D, Stefansson K (2011) Common variants at VRK2 and TCF4 conferring risk of schizophrenia. Hum Mol Genet 20: 4076-81. doi: 10.1093/hmg/ddr325

Stuart T, Butler A, Hoffman P, Hafemeister C, Papalexi E, Mauck WM, 3rd, Hao Y, Stoeckius M, Smibert P, Satija R (2019) Comprehensive Integration of Single-Cell Data. Cell 177: 1888-1902 e21. doi: 10.1016/j.cell.2019.05.031

Sun CP, Sun D, Luan ZL, Dai X, Bie X, Ming WH, Sun XW, Huo XX, Lu TL, Zhang D (2020) Association of SOX11 Polymorphisms in distal 3'UTR with Susceptibility for Schizophrenia. J Clin Lab Anal: e23306. doi: 10.1002/jcla.23306

Tomasch J (1954) Size, distribution, and number of fibres in the human corpus callosum. Anat Rec 119: 119-35. doi: 10.1002/ar.1091190109

Turan S, Boerstler T, Kavyanifar A, Loskarn S, Reis A, Winner B, Lie DC (2019) A novel human stem cell model for Coffin-Siris Syndrome like syndrome reveals the importance of SOX11 dosage for neuronal differentiation and survival. Hum Mol Genet. doi: 10.1093/hmg/ddz089

Tzeng M, du Souich C, Cheung HW, Boerkoel CF (2014) Coffin-Siris syndrome: phenotypic evolution of a novel SMARCA4 mutation. Am J Med Genet A 164A: 1808-14. doi: 10.1002/ajmg.a.36533

941 Wilson BJ, Harada R, LeDuy L, Hollenberg MD, Nepveu A (2009) CUX1 transcription
942 factor is a downstream effector of the proteinase-activated receptor 2 (PAR2). J Biol
943 Chem 284: 36-45. doi: 10.1074/jbc.M803808200

944 Zweier C, Peippo MM, Hoyer J, Sousa S, Bottani A, Clayton-Smith J, Reardon W,
945 Saraiva J, Cabral A, Gohring I, Devriendt K, de Ravel T, Bijlsma EK, Hennekam RC,
946 Orrico A, Cohen M, Dreweke A, Reis A, Nurnberg P, Rauch A (2007)
947 Haploinsufficiency of TCF4 causes syndromal mental retardation with intermittent
948 hyperventilation (Pitt-Hopkins syndrome). Am J Hum Genet 80: 994-1001. doi:
949 10.1086/515583

950

951

952

953

954

955

956

957

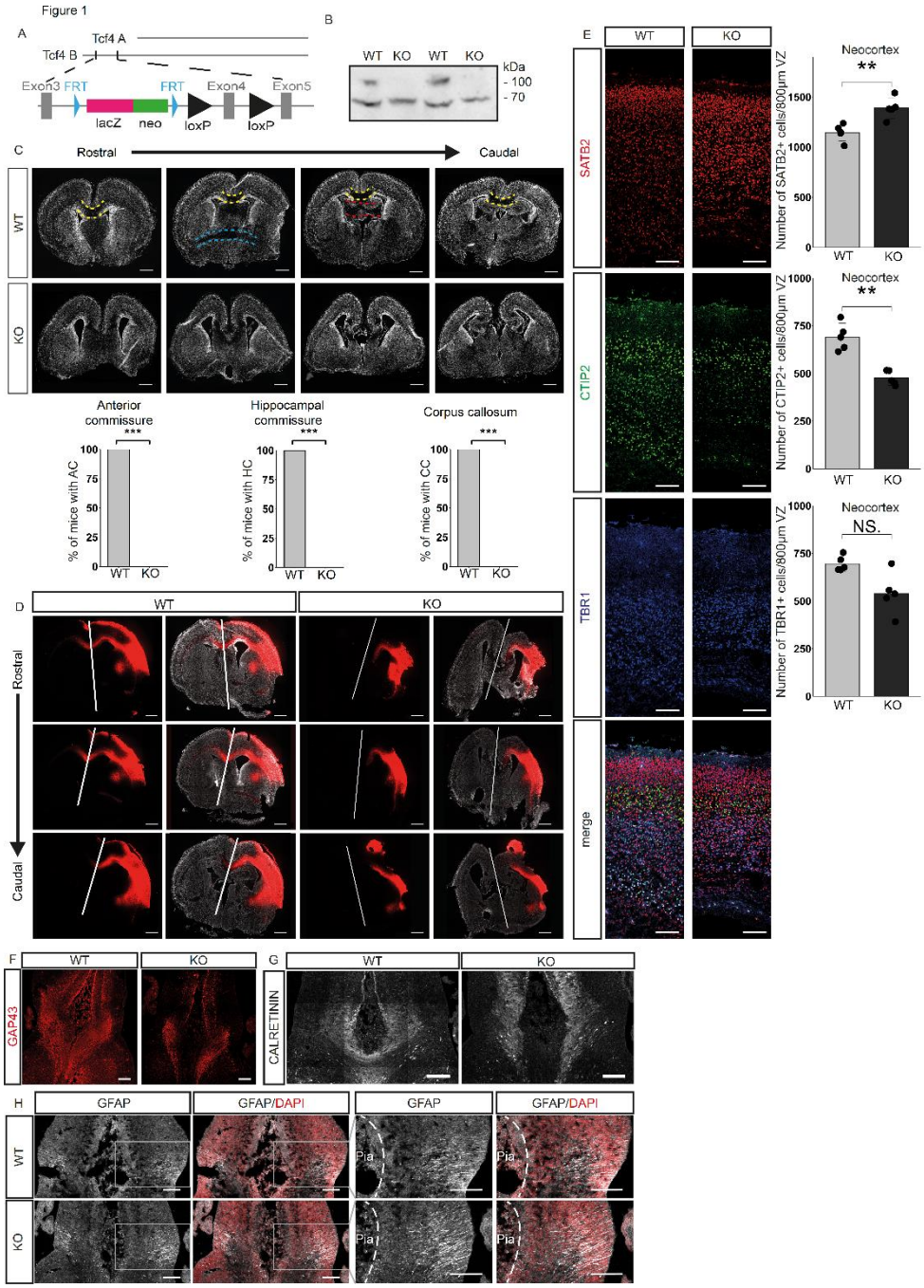

Figure 1. Loss of *Tcf4* disrupts cortex development, especially commissure formation

A Schematic representation of the two main *Tcf4* isoform and the `knockout-first´ conditional allele.
B Western Blot analysis of neocortical extracts from E18.5 WT or *Tcf4KO* mice using anti-TCF-4 antibody. The blot presented is cropped. The longest isoform of TCF-4 is missing in the KO samples (n = 3).
C Representative overview images (DAPI) of brain sections at P0 showing the loss of the three commissure systems in *Tcf4KO* mice. Yellow dotted lines indicate the CC crossing the midline. Blue dotted lines indicate the AC and red dotted lines the HC. Quantification of animals showing a commissural system is presented below (n = 8). Scale bar, 500 µm. Statistical significance was determined by two-tailed Mann-Whitney-U test (*, P ≤0.05; **, P ≤0.01, ***, P ≤0.001)
D Representative images of lipophilic tracer (red) treated brains at P0 without or with DAPI staining (white). White lines indicate the midline. Note that only in WT animals, lipophilic tracer signal can be detected in the contralateral hemispheres to the treatment (n = 3). Scale bar, 500 µm.
E Representative images of the neuronal markers SATB2 (upper layers), CTIP2 (layer V) and TBR1 (layer 6) and the quantification of the total cell number expressing these markers per 800µm ventricular zone (VZ). A significant increase in SATB2+ neurons is observable as is a significant decrease in CTIP2+ cells. Scale bar 100µm. Data is presented as mean ± SD; (n = 5). Statistical significance was determined by two-tailed Mann-Whitney-U test (*, P ≤0.05; **, P ≤0.01, ***, P ≤0.001).
F Representative images for GAP43 at the midline of E16.5 mouse brains. Scale bar, 100 µm, (n = 3).
G Representative images of CALRETININ expression at the midline at E16.5. Scale bar, 100 µm, (n = 3).
H Representative images of GFAP stainings at E16.5. Pictures on the right side are magnifications of the marked area. Dotted lines represent the pial surface. Scale bar, 100 µm, (n = 3).

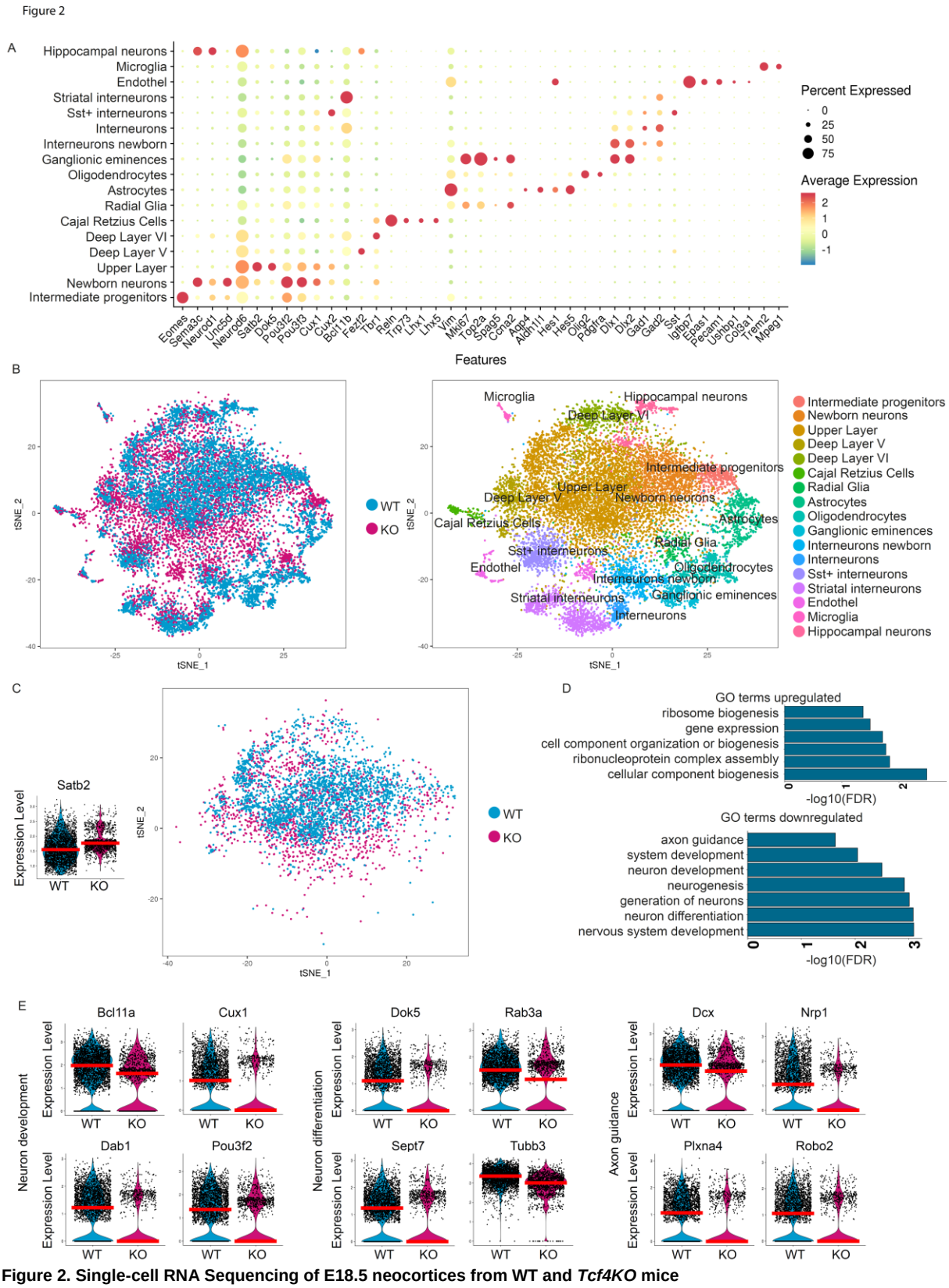

Figure 2. Single-cell RNA Sequencing of E18.5 neocortices from WT and *Tcf4KO* mice

A Dot-Plot of cell clusters (y-axis) and marker used to assign the cell type (x-axis).
B tSNE-Plot coloured by genotype (left) and cluster identity (right).
C tSNE-Plot of *Satb2* expressing glutamatergic cells used for further analysis. Violin Plot of *Satb2* expression in the *Satb2* cluster. The red line depicts the median.
D GO terms associated with up- and downregulated genes in SATB2 expressing glutamatergic cells. GO terms for neurogenesis, neuronal differentiation and axonogenesis were downregulated in the *Tcf4*KO cells.
E Violin Plot of differentially expressed genes in the *Satb2* cluster that are associated to neuron development/differentiation and axon guidance. The red line depicts the median.

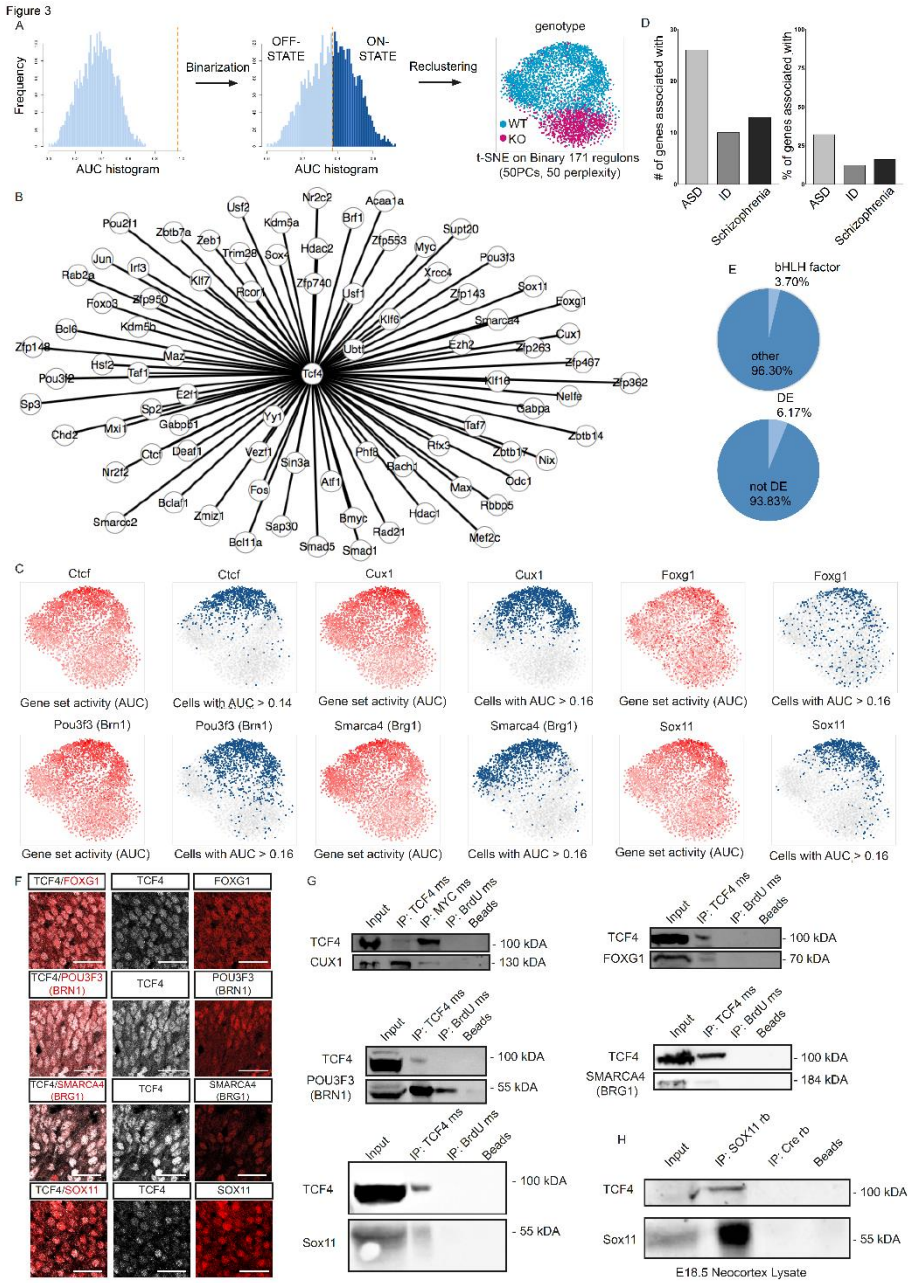

Figure 3. Gene regulatory network analysis of SATB2 expressing cells

A Scheme of the workflow used to recluster cells after GRN analysis and resulting tSNE-Plot of the *Satb2* cluster. Regulons are binarized and reclustered accordingly. WT and KO cells segregated based on GRN activity with only minor overlap.
B Differentially active regulons of the *Satb2* cluster that may be possible interactors of TCF-4.
C tSNE-Plots showing the regulon activity of *Ctcf, Cux1, Foxg1, Pou3f3* (also known as *Brn1*), *Smarca4* (also known as *Brg1*) and *Sox11* in a continuous scale (left, red) or binarized (right, blue). The regulons are preferentially active in the WT cells with only a small number of KO cells in the ON-State.
D Number and percentage of regulators associated with autism spectrum disorders (ASD), intellectual disability (ID) and schizophrenia in the *Satb2* cluster.
E Pie charts depicting the percentage of bHLH factors and differentially expressed regulators in the differentially active regulons.
F Representative images of TCF-4 (white) and FOXG1, POU3F3 (BRN1), SMARCA4 (BRG1) and SOX11 (all in red) in E18.5 WT cortices. Note the expression in the same nuclei. Scale bar, 50 µm
D Co-immunoprecipitation assay using anti-TCF-4 antibody conducted with HEK cell extract after overexpression of TCF-4 and CUX1, FOXG1, POU3F3 (BRN1), SMARCA4 (BRG1) and SOX11 in HEK cells. Upper panels: detection with anti-TCF-4 antibody. Lower panels: detection with anti-MYC, anti-FOXG1, anti-BRN1, anti-BRG1 or anti-SOX11 antibody. The blots presented are cropped. All proteins were co-immunoprecipitated with TCF-4, but not with an isotype control for IgG or Agarose A Beads alone except for BRN-1 which was precipitated to a small amount by the isotope control IgG. We could also show that TCF-4 was co-immunoprecipitated with anti-Myc antibody (precipitation of Myc-tagged Cux1). The interactions were confirmed in three independent biological replicates, (n = 3).
E Co-immunoprecipitation assay conducted with E18.5 cortex lysates using anti-SOX11 antibody. Upper panel: detection with anti-TCF-4 antibody. Lower panel: detection with anti-SOX11 antibody. The blots presented are cropped. TCF-4 was co-immunoprecipitated with SOX11, but not with an isotype control for IgG and Agarose A Beads alone. The interaction was confirmed in three independent biological replicates (n = 3).

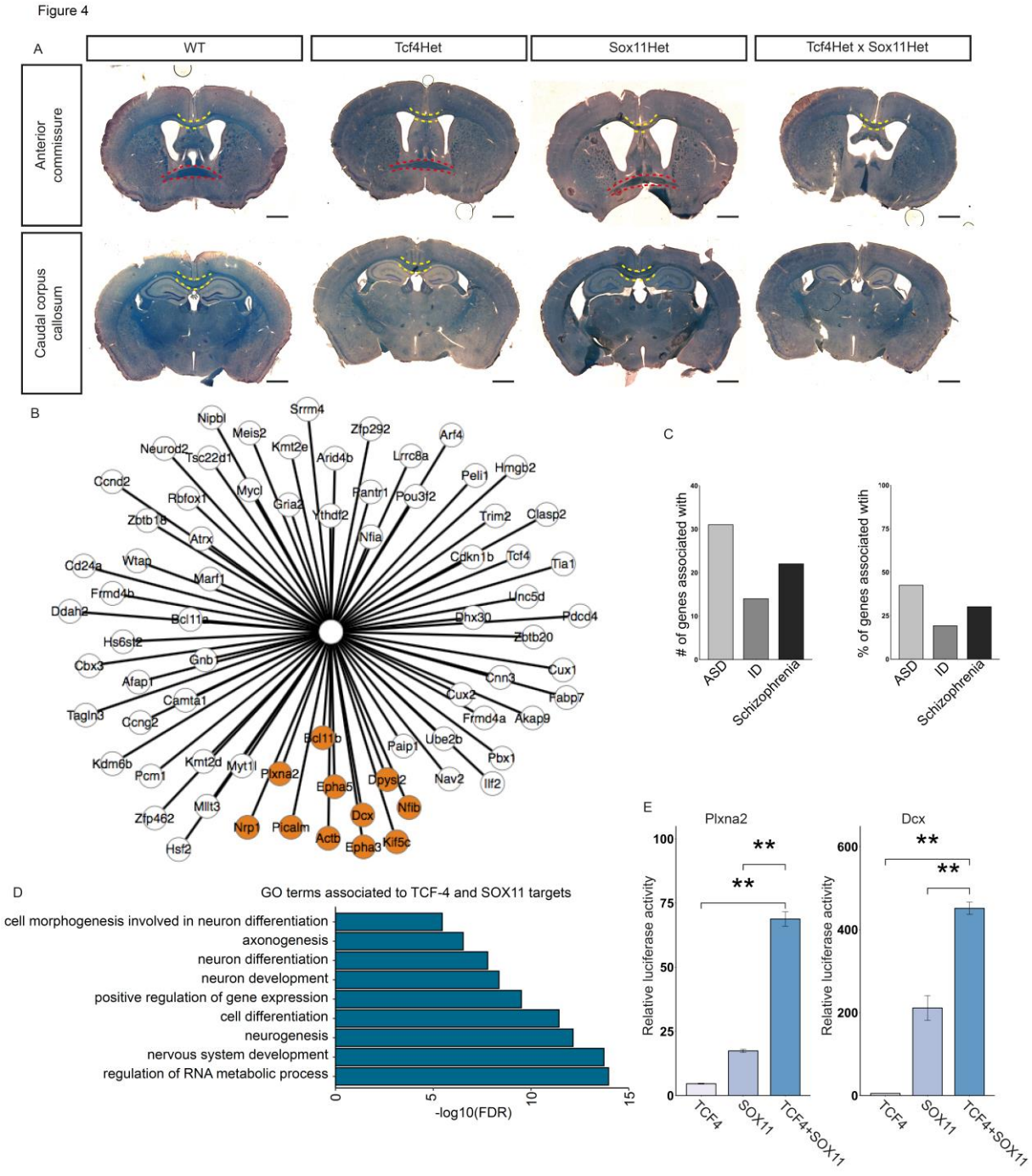

Figure 4. TCF-4 and SOX11 act synergistically in corpus callosum formation

A Representative overview images of Luxol fast blue stainings at the position of the AC and the caudal body of the CC. Yellow dotted lines indicate the CC crossing the midline. Red dotted lines indicate the AC. In *Tcf4* and *Sox11* double haploinsufficient mice agenesis of the AC and agenesis of the splenium and caudal part of the body of the CC can be observed. Scale bar, 1000 µm, (n=5).
B Common targets of TCF-4 and SOX11 in the *Satb2* cluster. Orange highlighted genes are associated with the GO term axonogenesis.
C Number and percentage of common targets of TCF-4 and SOX11 in the *Satb2* cluster associated to autism spectrum disorders (ASD), intellectual disability (ID) and schizophrenia in the *Satb2* cluster.
D Selection of GO terms associated with the common targets of TCF-4 and SOX11 in the *Satb2* cluster. GO terms for neurogenesis, neuronal differentiation and axonogenesis were enriched.
E Relative luciferase reporter gene activity under the control of the regulatory regions from the *Plxna2* (C) and *Dcx* (D) in transiently transfected HEK cells co-expressing TCF-4, SOX11 and a combination of the two (n = 3, presented as fold induction ± SD, transfection with empty CAG-GFP vector was set to 1 for each regulatory region). Statistical significance was determined by a two-tailed student´s t-test. (*, P ≤0.05; **, P ≤0.01, ***, P ≤0.001)

Supplement

Supplemental Dataset 1. Differential expressed genes in the Satb2 cluster and GO term analysis. Related to Figure 2.

Supplemental Dataset 2. Differential expressed genes in the limited Satb2 cluster and GO term analysis. Related to Figure 2.

Supplemental Dataset 3. Differential active regulons in the Satb2 cluster. Related to Figure 3.

Supplemental Dataset 4. Differential active regulons in the limited Satb2 cluster. Related to Figure 3.

Supplemental Dataset 5. Overlap of differential expressed genes and the predicted Sox11 regulon in the Satb2 cluster and GO term analysis. Related to Figure 4.